HHS Public Access

Author manuscript

*Colloids Surf B Biointerfaces*. Author manuscript; available in PMC 2020 January 01.

Published in final edited form as:

*Colloids Surf B Biointerfaces*. 2019 January 01; 173: 27–35. doi:10.1016/j.colsurfb.2018.09.047.

# Co-delivery of Doxorubicin and Erlotinib through Liposomal Nanoparticles for Glioblastoma Tumor Regression Using an *In Vitro* Brain Tumor Model

**Sushant Lakkadwala** and **Jagdish Singh***

Department of Pharmaceutical Sciences, School of Pharmacy, College of Health Professions, North Dakota State University, Fargo 58105, ND, USA

## Abstract

Glioma is a highly malignant tumor that starts in the glial cells of brain. Tumor cells reproduce quickly and infiltrate rapidly in high grade glioma. Permeability of chemotherapeutic agents into brain is restricted owing to the presence of blood brain barrier (BBB). In this study, we developed a dual functionalized liposomal delivery system for efficient transport of chemotherapeutics across BBB for the treatment of glioma. Liposomes were surface modified with transferrin (Tf) for receptor targeting, and cell penetrating peptide PFVYLI (PFV) to increase translocation of doxorubicin (Dox) and Erlotinib (Erlo) across the BBB into glioblastoma (U87) tumor cells. *In vitro* cytotoxicity and hemolysis studies were performed to assess biocompatibility of liposomal nanoparticles. Cellular uptake studies demonstrated efficient internalization of Dox and Erlo in U87, brain endothelial (bEnd.3), and glial cells. In addition, dual functionalized liposomes showed significantly ($p < 0.05$) higher apoptosis in U87 cells. Significantly ($p < 0.05$) higher translocation of dual functionalized liposomes across the BBB and delivering chemotherapeutic drugs to the glioblastoma tumor cells inside PLGA-Chitosan scaffold resulted in approximately 52% tumor cell death, using *in vitro* brain tumor model.

## Graphical Abstract

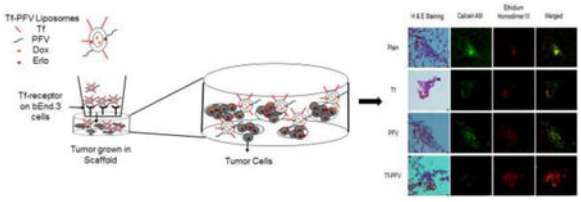


*Author to whom correspondence should be addressed; Department of Pharmaceutical Sciences, School of Pharmacy, College of Health Professions, North Dakota State University, Fargo 58105, ND, USA; jagdish.singh@ndsu.edu; Tel.: +1-701-231-7943; Fax: +1-701-231-8333.

Conflict of Interest

The authors declare no conflicts of interest.

**Keywords**

Dual-functionalized Liposomes; Glioblastoma; *In vitro* brain tumor model; Co-delivery; Blood brain barrier

## 1. Introduction

Glioblastoma multiforme (GBM) is an aggressive primary brain tumor of grade IV malignancy with poor prognosis. The tumor arises from astrocytes and is highly life threatening in nature due to rapid reproduction and infiltration of tumor cells into different parts of brain. Invasive nature of glioblastoma makes surgical removal of tumor difficult [1]. Available treatments include surgical resection, radiotherapy or chemotherapy are not able to increase the median survival time of 12–15 months [2,3]. Chemotherapy is the most common option for treatment of glioblastoma. However, presence of blood brain barrier (BBB) restricts the translocation of chemotherapeutic agents into the brain. Additionally, most chemotherapeutic agents cause undesirable effects due to inefficient targeting of tumor cells and toxic effects on healthy brain cells [4,5]. Therefore, it is warranted to develop an efficient glioblastoma targeting delivery system with high translocating ability across BBB as well as glioblastoma penetrating capabilities. We designed a dual functionalized liposomal system which could overcome all the aforementioned issues thereby delivering chemotherapeutic agents across BBB at high concentration to the core of tumor as well as migratory cells.

Transferrin receptors (TfR) are overexpressed on the surface of glioblastoma (U87) as well as on brain endothelial (bEnd.3) cells [6,7]. These TfR can be exploited for translocating a delivery carrier across the BBB [8–10]. In past years, sterically stable transferrin (Tf) coupled nanoparticles have been studied for delivering chemotherapeutic agents to the brain [11,12]. Receptor targeting delivery system could enhance the targeting effect of delivery carrier alone, however it was found to be limited due to receptor saturation [13,14]. In addition, it has been reported that the endocytic uptake of receptor targeting delivery system eventually leads to endosomal entrapment followed by degradation. Thus, to overcome the problem of endosomal entrapment, the surface of receptor targeting delivery system has been modified with cell penetrating peptides (CPPs) [15,16]. CPPs are short chain peptides which can facilitate intracellular uptake of delivery carriers. PFVYLI (PFV), is a synthetic peptide with only six amino acids which represents the c-terminal portion of C105Y [17]. This hydrophobic peptide sequence has shown potential in intracellular transport of delivery carriers [18–20]. In the present study, we evaluated anti-tumor efficacy of dual functionalized liposomes modified with Tf and PFV for co-delivery of doxorubicin (Dox) and erlotinib (Erlo), using *in vitro* brain tumor model.

The complex pathology of brain makes it one of the most complex organs of the human body. Due to this complex pathological nature of brain tumor, it is extremely difficult to develop an *in vitro* brain tumor model. Several models have been studied to imitate the complex pathology of brain tumor but none of them were able to address the presence of BBB, which is the major hurdle in transport of chemotherapeutics agents into the brain

[21,22]. In this study, we designed an *in vitro* brain tumor model by growing glioblastoma (U87) cells in a PLGA-chitosan porous scaffold to study the transport of dual-functionalized liposomes across endothelial barrier layer into 3-dimensionally grown tumor.

Combinational therapy of drugs has the potential to improve therapeutic efficacy by utilizing multiple non-overlapping and synergistic mechanisms, which thereby reducing the possibilities of drug resistance in cancer cells. Co-delivery of erlotinib, an epidermal growth factor receptor inhibitor, can extraordinarily synergize the apoptotic response to DNA damaging ability of doxorubicin. In this study, we modified the surface of liposomes with Tf for receptor targeting and PFV for enhanced cell penetration across BBB into brain. We evaluated *in vitro* biocompatibility of liposomal nanoparticles by using cell viability and hemolysis assay to determine their suitability for *in vivo* administration. We also performed *in vitro* cellular uptake and their mechanisms to determine the targeting and penetration ability of dual-functionalized liposomes. In addition, a detailed experimental investigation was performed to determine the transport and anti-tumor efficacy of Dox and Erlo encapsulated dual-functionalized liposomes by evaluating the transport across BBB, followed by increased accumulation of Dox and Erlo into tumor cells, resulting in tumor regression inside PLGA-chitosan scaffold using *in vitro* brain tumor model.

## 2. Materials and methods

### 2.1 Materials

1,2-dioleoyl-3-trimethylammonium-propane chloride (DOTAP), 1,2-dioleoyl-snglycero-3phosphoethanolamine-N-(lissamine rhodamine B sulfonyl) (DOPE-lissamine rhodamine), and 1,2dioleoyl-sn-glycero-3-phosphoethanolamine (DOPE) were purchased from Avanti Polar Limited (Birmingham, Alabama). 3-(N-succinimidyloxyglutaryl) aminopropyl, polyethyleneglycol-carbamyl distearoylphosphatidyl-ethanolamine (NHS-$PEG_{(2000)}$-DSPE) was obtained from Biochempeg Scientific Inc. (Watertown, Massachusetts). Doxorubicin HCl was procured from MedChem Express (Monmouth Junction, New Jersey). Erlotinib was obtained from Cambridge Chemicals (Woburn, Massachusetts). Transferrin (Tf), Cholesterol (Chol) and Chitosan (50 kDa) were procured from Sigma-Aldrich Company (St. Louis, Missouri). PFVYLI (PFV) was obtained from Zhejiang Ontores Biotechnologies Co., Ltd (Zhejiang, China). Fetal bovine serum (FBS) was purchased from Omega scientific Inc. (Tarzana, California). Dulbecco's modified eagle medium (DMEM) and Dulbecco's phosphate buffered saline (DPBS) were obtained from Mediatech Inc. (Manassas, Virginia). 3-(4, 5-dimethylthiazol-2-yl)-2, 5- diphenyltetrazolium bromide (MTT) was purchased from Alfa Aesar (Ward Hill, Massachusetts). Polyethylene terephthalate (PET) thincerts, cell culture inserts were procured from Greiner Bio-One International (Monroe, North Carolina). FITC Annexin V Apoptosis detection kit was purchased from BD Biosciences (San Diego, California). Poly (D, L-lactide-co-glycolide) 50:50 was obtained from Polyscitech (West Lafayette, Indiana). All the chemicals used were of analytical grade. Brain endothelial cells (bEnd.3) were obtained from American Type Culture Collection (ATCC, Rockville, Maryland).

## 2.2 Synthesis of PFV-PEG$_{(2000)}$-DSPE and Tf-PEG$_{(2000)}$-DSPE:

**2.2.1 Synthesis of PFV-PEG$_{(2000)}$-DSPE:** PFV was coupled to the terminal end of activated NHS-PEG$_{(2000)}$-DSPE using nucleophilic substitution reaction as previously described [19]. Briefly, NHSPEG$_{(2000)}$-DSPE and PFV were dissolved at a molar ratio 4:1 in an anhydrous dimethylformamide (DMF). The pH of the solution was adjusted between 8–9 using trimethylamine and stirred for 3 days at room temperature. The free uncoupled PFA was removed through dialysis membrane MWCO 3.5kDa for 48 h. The final product was lyophilized and stored at −20º C until used. The coupling efficiency was determined using HPLC at a wavelength at 220 nm using MOS-1 hypersil column (Thermoscientific, 5 μm, 250 × 4.6 mm).

**2.2.2 Synthesis of Tf-PEG$_{(2000)}$-DSPE:** Tf was coupled to the distal end of to NHS-PEG$_{(2000)}$-DSPE using nucleophilic substitution, as described in the previous section [12,23]. Briefly, NHS-PEG$_{(2000)}$DSPE and Tf (125 μg /μ mole of phospholipid) was dissolved in an anhydrous DMF. The pH of the solution was further adjusted between 8–9 using trimethylamine and stirred for 24 h at room temperature. Uncoupled transferrin was separated by passing through G-100 sephadex. The coupling efficiency was determined by microBCA. Briefly, 400 μl of methanol was mixed with 100 μl of liposomal suspension, vortexed and centrifuged for 30 s at 9000 × g. Further, 200 μl of chloroform was added to this mixture, vortexed and centrifuged at 9000 × g for 30 s. Then 300 μl of water was added which led to phase separation. The mixture was further vortexed and centrifuged for 1 min at 9000 × g. After discarding supernatant, 200 μl of methanol was added to the interphase between chloroform and protein precipitate. Thereafter, the mixture was again vortexed and centrifuged at 9000 × g for 2 mins. The upper layer was discarded and protein pellet was air dried. The dried protein pellet was dissolved in 100 μl of phosphate buffer saline (PBS), pH 7.4 and analyzed using micro BCA assay as per the manufacturer's protocol in order to determine coupling efficiency.

## 2.3 Preparation of Dual Functionalized Liposomes and Drug Loading:

The dual-functionalized liposomes were prepared using thin film hydration and post-insertion technique [12]. Briefly, erlotinib and PFV-PEG$_{(2000)}$-DSPE along with other phospholipids were dissolved in chloroform: methanol (2:1 (v/v)), in the following molar ratio: DOTAP/DOPE/Chol/PFV-PEG$_{(2000)}$-DSPE (45:45:2:4 mole %). The solvent mixture was evaporated using rotavapor (Buchi Rotavapor RII, New Castle, DE) to form a thin lipid film. Then, the dried lipid film was hydrated with 300 mM citric acid buffer, pH 5.0 to form PFV coupled liposomes. The Tf-PEG$_{(2000)}$-DSPE micelles were stirred overnight at room temperature with PFV-liposomes to form dual functionalized liposomes (Tf-PFVliposomes). To encapsulate doxorubicin into liposomes, reported pH gradient method was used, with some modifications [12]. Tf-PFV liposomes were titrated with 300 mM sodium carbonate to create pH gradient. Doxorubicin was added to the preformed liposomes and incubated at 50°C for 1 h. Then, the drug loaded liposomes were cooled down to room temperature and subsequently passed through sephedex G-100 column to remove unentrapped drug. The final functionalized liposomes (Tf-PFV liposomes) were passed through sterile 0.2 μm filter. The liposomal nanoparticles were stored at 4ºC and used within 48 h of preparation.

The entrapment efficiency of drugs was quantified using high performance liquid chromatography (HPLC). Briefly, 100 μl of liposomal formulation before and after passing through the sephedex G-100 column, was mixed with 200 μl D.I. water along with 100 μl of methanol and 100 μl of triton X100 (0.5% v/v). Then, this dispersion was centrifuged at 3000 rpm for 10 min and the supernatant was injected into HPLC. Dox analysis was performed at a wavelength of 234 nm using C-18 column (Thermoscientific Hypersil Gold, 5 μm, 250 × 4.6 mm) and mobile phase consisted of 0.2 M phosphate buffer, pH 5.5 : acetonitrile (70:30) with a flow rate of 1 ml/min at room temperature, with some modifications [12]. Erlo was analyzed at a wavelength of 246 nm using C-8 column (Thermoscientific Hypersil BDS, 5 μm, 250 × 4.6 mm) and mobile phase consisting 0.2 M potassium phosphate, pH 3.0: acetonitrile (50:50) with a flow rate of 0.750 ml/min at room temperature, with some modifications [24].

For preparation of lissamine-rhodamine and coumarin-6 labeled liposomes, the lipid mixture was added with 0.5 mole% of dye along with other lipids prior to formation of thin lipid film.

### 2.4 Size and Zeta Potential of Liposomal Nanoparticles:

The hydrodynamic diameter and zeta potential of the liposomes were measured by zetasizer ZS 90 (Malvern Instruments, Worcestershire, UK) after appropriately diluted with PBS. The sample filled cuvettes were placed in the path of 5 mW He−Ne laser of wavelength 633 nm at 25ºC. The data was collected at a scattering angle of 90º.

### 2.5 *In vitro* Release of Doxorubicin and Erlotinib:

*In vitro* release studies of doxorubicin and erlotinib were performed by diluting liposomes in phosphate buffer saline (PBS, pH 7.4) with 10% FBS. The drugs encapsulated liposomes were placed into a dialysis tube (MWCO 6000–8000) and tightly sealed. Then, the dialysis tube was immersed into 50 ml of phosphate buffer saline (PBS, pH 7.4) and incubated at 37 ± 0.5°C with mild oscillation of 50 rpm. At predetermined intervals, 1 ml of samples were taken and replaced with same volume of fresh PBS (pH 7.4). The samples were analyzed using HPLC, as described above for evaluation of doxorubicin and erlotinib loading.

### 2.6 *In Vitro* Biocompatibility:

The cationic nature of the CPP may cause cell toxicity [18]. In this study, the cytotoxic potential of drug-free liposomes of different concentrations of phospholipids in U87, bEnd. 3, and glial cell lines was studied using MTT assay. Briefly, 1,000 cells per well were seeded in 96 well plates in 200 μl of DMEM supplemented with 10% FBS and 1% pen-strep and incubated at 37ºC under 5% $CO_2$ atmosphere. After attachment for 24 h, different phospholipid concentrations of drug-free liposomes (plain, Tf, PFV, and Tf-PFV liposomes) in serum free media were added to the wells and incubated for 2 h. Subsequently, the formulation was removed and replaced with fresh serum containing media. The cells were further incubated at 37ºC under 5% $CO_2$ atmosphere, for 48 h. Cell viability was then evaluated by MTT assay [12]. Untreated cells were considered as control group under the same cell culture conditions.

### 2.7 Cellular uptake Assessment:

U87, bEnd.3 and glial cells were seeded in 6 well plate at a density of 6 X $10^5$ cells per well and incubated at 37°C under 5% $CO_2$ atmosphere. After attachment of 24 h, different Dox and Erlo encapsulated liposomal formulations were added in each well at a concentration of 200 nMoles of phospholipid and cellular uptake was studied for 2 h. After treatment, the cells were washed and rinsed with DPBS, PH 7.4. The nuclei of cell was stained with 1 ml of Hoechst 33342 (1 μg/mL). Then, the cells were observed under Leica DMi8 fluorescence microscope (Leica Microsystems Inc., Buffalo Grove, IL). For quantitative uptake of Dox and Erlo, the cells were lyzed in triton x-100 (0.5% v/v) followed by extraction of drugs by addition of methanol to the cell lysate. Then, the solution was centrifuged at 10,000 rpm for 15 min at 4°C and the supernatant was injected in HPLC. The analysis was performed as described previously for quantification of Dox and Erlo entrapped into liposomes.

### 2.8 Evaluation of Endocytosis Pathways:

To elucidate the endocytosis pathways of liposomes, various membrane inhibitors were used. The cells (U87, bEnd.3, and glial cells) were seeded in 6 well plate at a density of 6 X $10^5$ cells per well. After attachment for 24 h, the cells were incubated at 4°C to inhibit all energy dependent endocytic pathways [25] or pre-incubated cells for 30 min with either colchicine (10 μM) inhibits the formation of caveolae [26], methyl-β-cyclodextrin (5 mM) prevents cholesterol dependent endocytic processes [27], chlorpromazine (10 μ g/ml) inhibits the development of clathrin-coated vesicles [25], or amiloride (50 μM) prevents macropinocytes [28], followed by incubation of coumarin-6 loaded liposomes (200 nMoles of phospholipid concentration) for 2 h. Subsequently, the cells were washed and lyzed by adding 50 μl of triton X-100 (0.5% v/v) followed by adding 450 μl of methanol to extract coumarin-6. The cell lysate was centrifuged at 10,000 rpm for 15 min at 4°C. Then, the supernatant was assessed by measuring the fluorescence intensity of coumarin-6 using fluorescence SpectraMax® M5 spectrophotometer microplate reader (excitation wavelength = 465 nm, emission wavelength: 502 nm). The cells without treated with inhibitors were used a controls.

### 2.9 Apoptosis Study:

FITC-annexin-V/ propidium iodide (PI) double staining assay was used to quantify the apoptosis in U87 cells by liposomal formulations. Briefly, 1 × $10^6$ cells per well were seeded in 6 wells plates. After attachment for 24 h, the cells were incubated with different Dox and Erlo loaded liposomes and free Dox-Erlo for 5 hours. Then, the formulations were replaced with fresh complete medium and incubated under same cell culture conditions for 24 h. Consequently, the cells were washed, collected by trypsinization, and stained with Annexin V-FITC apoptosis detection kit. The cells were immediately assessed in accordance with manufacturer's protocol, using BD Accuri C6 flow cytometer (BD Biosciences Accuri cytometers, San Jose, CA).

### 2.10 Hemolysis Study:

The liposomes in the present study are meant to be injected intravenously and can interact with negatively charged erythrocytes membrane which may cause hemolysis. Therefore, *in*

*vitro* hemolysis test is warranted prior to *in vivo* study. Briefly, blood was collected into EDTA containing tubes from an adult rat and centrifuged at 2000 rpm for 10 min. Then, the obtained pellet was washed thrice with sterile PBS, pH 7.4. Different phospholipid concentrations of liposomes were incubated with $1.5 \times 10^7$ number of erythrocytes for 60 min at 37°C. Consequently, the samples were centrifuged at 2000 rpm for 10 min and absorbance of the supernatant was determined at 540 nm using spectrophotometer (SpectraMax® M5, Molecular devices, Sunnyvale, CA). Erythrocytes hemolysis of 100% and 0% after treatment with triton x-100 and PBS were taken as controls, respectively. Less than 10% of hemolysis was considered non-toxic [29,30]. The percent hemolysis was calculated by using the following equation:[12,31]

$$\text{Percent hemolysis} = \left[\left(\text{Abs}_{(\text{treatment})} - \text{Abs}_{(\text{PBS})}\right) / \text{Abs}_{(\text{Triton x} - 100)}\right] \text{x } 100$$

Where $\text{Abs}_{(\text{treatment})}$, $\text{Abs}_{(\text{PBS})}$ and $\text{Abs}_{(\text{T})}$ are the absorbance of treatment groups, PBS and triton x-100, respectively.

## 2.11 Design of Endothelial Barrier:

The *in vitro* endothelial barrier was constructed according to previously published reports [12,32,33]. Briefly, the co-culture barrier was formed by seeding bEnd.3 cells (37,500 cells/$cm^2$) and glial cells (15,000 cells/$cm^2$) on luminal side and abluminal side of the insert, respectively. The media of barrier was replaced with fresh media every 2 days and cells were checked for confluency. The integrity of the barrier was assessed by measuring the flux of sodium fluorescein (Na-F) across the co-culture barrier layer [12] as well as by measuring the transendothelial electrical resistance (TEER) using EVOM2 with STX2 (World Precision Instruments, Sarasota, FL) [32]. The Na-F permeability across both co-culture (bEnd.3 and glial cells) and monolayer (only bEnd.3 cells) barrier was determined by replacing the medium with 500 µl containing 10 µg/ml Na-F in the upper compartment of the culture insert and 1 ml of DPBS in the lower compartment of the 24 well plates. At predetermined time points, samples were taken by transferring the culture insert to new wells containing 1 ml DPBS. Then, the fluorescence intensity of Na-F was measured using spectrophotometer (SpectraMax® M5, Molecular devices, Sunnyvale, CA) at excitation/emission wavelengths of 485/535 nm, respectively. The following equation was used to calculate the endothelial permeability coefficient ($P_e$): [13,34,35]

$$1/P_e = 1/P_t - 1/P_f \text{ cm/s}$$

where, $P_t$ is the apparent permeability coefficient across the total barrier model while $P_f$ is the apparent permeability coefficient across cell free culture insert.

## 2.12 Growth of Tumor Cells Inside PLGA-Chitosan Scaffold:

The scaffold was prepared using emulsion freeze dry method as previously reported [12,35]. Briefly, 0.2 g of poly (D, L-lactide-coglycolide) (50:50) (PLGA) was dissolved in 1 ml of dichloromethane. Separately, chitosan (500 mg) and polyvinyl alcohol (PVA, 150 mg) were dissolved in 10 ml of acetic acid buffer, pH 4.5. An emulsified paste was prepared by slowly

adding and stirring the PLGA solution to chitosan-PVA mixture. Then, 500 μl of collagen solution (0.1% w/v) was added to this emulsified paste and poured into a rod shaped mold and freeze dried. Before seeding U87 cells, the scaffolds were cut into 2mm circular disc and then treated with 70% ethanol. Thereafter, the scaffolds were soaked with DMEM supplemented with 30% FBS overnight. Following day, $5 \times 10^5$ U87 cells were seeded on the surface of scaffold and incubated for 6 h, followed by addition of fresh media supplemented with 30% FBS. The media surrounded by scaffold was replaced with fresh media every other day. At different time points, the growth of the U87 tumor cells inside scaffolds was monitored using hematoxylin eosin staining.

### 2.13 Assessment of Liposomal Transport:

To evaluate the transport of liposomes across *in vitro* brain tumor model, the model was constructed by placing the co-culture (bEnd.3 and glial cells) endothelial barrier above the glioblastoma grown scaffold on day 14 and further cultured for 7 days. This model was constructed to simulate *in vivo* like conditions, where the liposomes have to first translocate across the co-culture barrier before reaching to the glioblastoma tumor site inside the scaffold. The transport of drug loaded liposomes was quantified across the *in vitro* brain tumor model. The transport was carried out in sterile DPBS containing 10% FBS to mimic the *in vivo* condition. The co-culture endothelial barrier was placed on glioblastoma grown scaffold in 24 well plates containing 1ml of DPBS with 10% FBS. Different liposomal formulations (200 nMoles of phospholipid concentration) in 500 μl of fresh serum containing buffer were added in the upper compartment of the co-culture barrier insert. The liposomes were transported across the co-culture endothelial barrier into the 3-dimensional glioblastoma tumor grown scaffold. Then, tumor cells were lyzed as described above and the lysate was analyzed as the same way described in the cellular uptake study using HPLC.

### 2.14 Anti-Tumor Efficacy of Liposomes:

To assess antitumor efficacy of liposomes, *in vitro* brain tumor model was used, as constructed in previous section. On day 21 of tumor growth, the model was treated with different Dox and Erlo loaded liposomal formulations. Briefly, the media surrounding by the tumor scaffold was replaced by fresh serum containing DPBS pH 7.4. The media in the upper compartment of co-culture barrier insert was replaced with Dox and Erlo loaded liposomal nanoparticles (200 nMoles of phospholipid concentration) and free drugs (Dox (10 μg) and Erlo (8 μg)) in 500 μl of fresh serum containing DPBS and treated for 24 h. After treatment, the scaffold was incubated at 37°C under 5% $CO_2$ atmosphere in fresh media containing 30% FBS for 6 more days. The media surrounded by scaffold was replaced with fresh media in every 2 days and percent cell viability was quantified using MTT assay. For fluorescence imaging, the treated scaffolds were stained with live/dead cell staining (Biotum Inc., Fremont, CA) according to the manufacturer's protocol. Then, the scaffolds were embedded in OCT and snap frozen. With the help of cryostat, 20 μm thick sections of scaffolds were cut and stained with hematoxylin-eosin staining. The fluorescence images of scaffolds were observed using Leica DMi8 fluorescence microscope (Leica Microsystems Inc., Buffalo Grove, IL).

### 2.15 Data Analysis:

All the quantitative data were demonstrated as a mean ± standard deviation (S.D.). Statistical significant analysis among groups were performed using either Student's t test, one or two-way ANOVA. A P value of less than 0.05 was considered statistically significant. All quantitative data analysis was performed using Graphpad Prime 5.0 for windows (GraphPad Software, Inc., La Jolla, CA).

## 3. Results and discussion

### 3.1 Synthesis of PFV peptide and Tf with NHS-PEG$_{(2000)}$-DSPE:

Tf and PFV were successfully coupled to the distal end of the NHS-PEG$_{(2000)}$ –DSPE through nucleophilic substitution reaction in the presence of trimethylamine (Fig. 1A). The amine groups present in Tf bind covalently to the distal terminal of PEG derivatives, which was confirmed by micro BCA assay and showed a coupling efficiency of 83.02 ± 4.38 %. Moreover, the PFV conjugation to NHS-PEG$_{(2000)}$-DSPE was confirmed by HPLC by monitoring the reaction until the constant peak of PFV was achieved. As shown in Fig. 1B, the retention time of PFV was approximately 26 min, and the coupling efficiency was approximately 81% after 3 days. This indicates that PFV present in the reaction mixture, has been coupled to the NHS-PEG$_{(2000)}$-DSPE.

### 3.2 Characterization of Liposomes:

The mean particle size of various liposomes was found in the range of 158.7 to 165.05 nm (Table 1). Therefore, surface modification of liposomes with Tf and PFV did not show any significant difference ($p > 0.05$) in particle sizes. The polydispersity index (PDI) of various liposomes were less than 0.232, showing highly uniform liposomal particles. A particle size distribution graph of Tf-PFV liposomes is shown in Fig. S1A. The zeta potential of plain and Tf-PFV liposomes was observed to be 5.33 ± 0.66 and 7.66 ± 0.87 mV. The results indicate that the conjugation of negatively charged transferrin has changed the net charge on liposomes to a negative value. However, the Tf-PFV liposomes have near neutral charge (0–15 mV), which can be explained by the counter balancing of negatively charge Tf with the positively charge PFV. The size and zeta potential are important factors in determining the stability of colloidal suspension during storage. The incorporation of polyethylene glycol, a stearic stabilizer helps in reducing aggregation of liposomes and improving their stability during storage [31]. The entrapment efficiency of Dox and Erlo for all liposomal formulations were found to be approximately 65 % and 54 %, respectively and demonstrated no significant difference in the entrapment of drugs amongst different liposomal formulations. The *in vitro* release profile of Dox and Erlo loaded liposomes were studied in 10% FBS. The percent cumulative release for Dox and Erlo was more than 30% and 32% for liposomes, respectively, over the period of 24 h (Fig. S1B and C).

### 3.3 *In Vitro* Biocompatibility of Liposomes:

*In vitro* biocompatibility of liposomes was studied by using MTT assay in glioblastoma (U87), brain endothelial (bEnd.3), and primary glial cell lines to demonstrate that liposomes are non-toxic and biocompatible. It is also important to determine an optimal concentration

of delivery carrier and its ability to release encapsulated content in a safe and effective way. The results revealed cell viability of more than 85% compared to control, after exposure to liposomes up to a phospholipid concentration of 200 nMoles. The cell viabilities at 600 nMoles concentration were found to be 70.51 ± 1.68%, 67.58 ± 1.99%, and 71.24 ± 1.70% in U87, bEnd.3, and primary glial cell lines, respectively. Moreover, there was a decrease in cell viability with increasing concentration of phospholipid (Fig. 2). Irrespective of the type of cells, the cell viability of positively charge PFV-liposomes was lower ($p > 0.05$) compared to the negatively charge Tf-liposomes, Tf-PFV liposomes, and plain liposomes (Fig. 2), which may be attributed to the higher positive charge of PFV on the surface of liposomes.

### 3.4 Cellular Uptake:

The cellular uptake of various liposomal formulations was studied qualitatively as well as quantitatively in three different type of cells. As depicted in the Fig S2, Tf-PFV liposomes labeled with lissamine rhodamine showed maximum uptake. The fluorescence images corroborate the strong pattern of lissamine rhodamine fluorescence throughout the cytoplasm as well as in the nucleus, indicating a significantly higher cellular uptake as compared to single-ligand or plain liposomes in all the three types of cells. The quantitative estimation of Dox and Erlo cellular uptake further confirmed the efficacy of Tf-PFV liposomes uptake in different type of cells (Fig. 3A and B). The Dox uptake from the Tf-PFV liposomes showed approximately 66%, 66%, and 65% in U87, bEnd.3, and Primary glial cells, respectively. Furthermore, the uptake of Tf-PFV liposomes encapsulating Erlo was found to be approximately 69%, 68%, and 64% in U87, bEnd.3, and primary glial cells, respectively. The Tf-PFV liposomes showed significantly higher ($p < 0.05$) cellular uptake compared to single ligand or plain liposomes. The cellular uptake of Tf-liposomes was not significantly higher than PFV-liposomes, which explained that the greater uptake through receptormediated transcytosis. Moreover, the high electrostatic interaction between the heparin sulfate proteoglycans present on the surface of cell membrane and cationic PFV enables the higher cellular uptake of liposomes. Therefore, Tf-PFV liposomes exhibited the synergistic cellular uptake of liposomes by adsorptive and Tf receptor facilitated transcytosis. In addition, the cellular uptake of Tf-PFV liposomes demonstrated higher uptake in U87 compared to bEnd.3 and primary glial cells. Thus, the rate of cellular uptake is dependent on the type of cells [12]. In conclusion, the results demonstrated the significance of dual modifications of liposomes over receptor-mediated or cell penetration.

### 3.5 Cellular Uptake Mechanism:

To elucidate the pathways involved in cellular uptake of Tf-PFV liposomes, several endocytosis inhibitors were used. Fig. 4 shows the findings of the effect of these inhibitors on cellular uptake of coumarin-6 from the various liposomal formulations. When temperature changed from 37°C to 4°C, the cellular uptake reduced in all the three types of cells, which shows the uptake of Tf-PFV liposomes is energy-dependent. When cells were pretreated with colchicine, an inhibitor of caveolae formation, which specifically blocks caveolar mediated endocytosis, revealed no obvious inhibition on cellular uptake of Plain, Tf, PFV, and Tf-PFV liposomes. Methyl-β-cyclodextrin (M-β CD) blocks the endocytosis pathway via cholesterol depletion, which resulted in significant decrease in the uptake of liposomes [12,19,36]. In addition, during the process of cellular uptake, cholesterol involves

in the formation of cavities which ultimately lead to the development of clathrin-coated vesicles. Chlorpromazine (CPZ), a specific inhibitor of clathrin-mediated endocytosis, indicated significant reduction in the cellular uptake, thereby demonstrating major pathway for cellular uptake of liposomes [12,19,37]. Amiloride can interfere in the uptake of liposomes via macropinocytosis, by inhibition of sodium-proton exchange [38]. However, amiloride did not significantly inhibit the liposomal uptake, thereby eliminating the macropinocytosis as the uptake pathway. Therefore, it can be concluded from the results that liposomes were transported primarily through clathrin-mediated endocytosis as well as clathrin-coated vesicles.

### 3.6 Apoptosis Assessment:

As depicted in Fig. 5A and S3, the exposure of various liposomes resulted in the apoptosis of U87 cells. The total percentage apoptosis in U87 cells was about 60.87 ± 6.57, 45.62 ± 1.28, 45.67 ± 1.99, 36.02 ±1.41, 24.32 ± 2.78 and 11.87 ± 0.71 for Tf-PFV, PFV, Tf, Plain liposomes, Free Dox-Erlo, and control, respectively. Incubation of U87 cells with Tf-PFV liposomes containing Dox and Erlo demonstrated enhanced U87 cell apoptosis compared to plain liposomes containing Dox and Erlo. Therefore, based on the apoptotic assay, it can be concluded that Dox-Erlo loaded liposomes showed significantly ($p < 0.05$) higher apoptotic effect when the liposomal surface was modified with Tf and PFV.

### 3.7 Hemolysis Study:

It is critical to study liposomes biocompatibility for *in vivo* administration. To elucidate *in vitro* biocompatibility, hemolysis study was performed to get an insight into the interaction of cationic charged liposomes with negatively charged erythrocytes' membrane, which triggers thrombosis, embolization or hemolysis, *in vivo* [31,39,40]. Such interaction can lyse the erythrocytes and release hemoglobin. It was found that increase in phospholipid concentrations lead to a higher release of hemoglobin from the erythrocytes (Fig. 5B). The results showed that percent hemolysis for Tf-PFV liposomes was less than 6% at 600 nMoles phospholipid concentration. In general, upto 10% of hemolysis is considered as non-toxic and biocompatible [41]. Therefore, it can be concluded that Tf-PFV liposomes are non-toxic and biocompatible for *in vivo* administration.

### 3.8 *In Vitro* BBB Integrity and 3D Tumor Model:

The integrity of BBB was assessed by measuring the flux of sodium fluorescence (Na-F) and TEER across the co-culture of bEnd.3 cells and glial cells. The integrity of endothelial cells associated glial cells determined the intactness of the endothelial barrier layer. We observed significant ($p < 0.05$) decrease in the paracellular transport of Na-F across the co-culture model with bEnd.3 and glial cell ($Pe = 2.17 \times 10^{-6}$ cm/s) as compared to monolayer model ($Pe = 11.7 \times 10^{-6}$ cm/s) (Fig. S4A). The lower permeability coefficient of Na-F across coculture model attributed to the physical contact between the endothelial and glial cells, thereby showing improved complex between junctional proteins, showing the significance of glial cells in the formation of tight BBB [12,13,42,43]. Likewise, the TEER across co-culture and monolayer models was also determined to confirm the intactness of the endothelial barrier. The TEER values of both monolayer and co-culture model were observed to be increasing with increase in the cell densities. The TEER value for the co-

cultured model after 6 days of incubation period, was found to be 178.4 ± 10 Ω $cm^2$, significantly ($p < 0.05$) higher compared to 110.6 ± 3.5 Ω $cm^2$ for the monolayer model (Fig. S4B). This can be explained by the up regulation of junctional proteins in the co-cultured model and supported by the presence of glial cells, which make a tighter barrier [44]. In addition, Microscopic images of hematoxylin-eosin stained scaffold sections showed gradual growth of U87 tumor cells as depicted in Fig. 6A. The images of scaffold with tumor cells exhibited cellular biocompatibility. In addition, the porous nature of scaffold facilitates the attachment of tumor cells, thus supporting the tumor growth in 3-dimensional environment [45]. On day 21, the histological images of scaffold demonstrated dense growth of tumor cells inside the scaffolds.

### 3.9 Transport of Liposomes Across *In Vitro* Brain Tumor Model:

In this study, we developed an *in vitro* brain tumor model to study the transport of Tf-PFV liposomes across the endothelial barrier layer into tumor grown in the porous PLGA-chitosan scaffold. The model was prepared by culturing glioblastoma cells in the porous PLGA-chitosan scaffold and combining it with co-cultured endothelial barrier, thereby mimicked *in vivo* like conditions. Moreover, the endothelial barrier layer was constructed by culturing glial and bEnd.3 cells on the abluminal and luminal side of PET membrane of insert, respectively. The transport study was performed using 10% serum to create *in vivo* like condition, thus eliminating the chances of liposomes entrapped into the endothelial barrier layer. The drug loaded Tf-PFV liposomes demonstrated significantly ($p < 0.05$) higher transport across the *in vitro* brain tumor model as compared to single ligand or plain liposomes alone. The percent liposomal transport was increased from 8.05% and 8.7% for Tf and PFV liposomes to 12.67% for Tf-PFV over a period of 24 h (Fig. 6B). Thus, the Tf-liposomes transported after binding to transferrin receptor via receptor mediated transcytosis, whereas the electrostatic binding of the cationic charged PFV-liposomes with negatively charged cell membrane facilitates the transport across the endothelial barrier. Therefore, Tf-PFV liposomes efficiently transported through dual mechanisms of receptor mediated transcytosis and cell penetration across the *in vitro* BBB model.

### 3.10 Anti-Tumor Efficacy:

The antitumor efficacy of Tf-PFV liposomes was studied by quantifying the percent tumor cell viability in scaffold using MTT assay as well as determining qualitatively using live/dead cell imaging using *in vitro* brain tumor model. The tightly packed endothelial barrier layer (co-culture model) combined with U87 housed PLGA-chitosan scaffold, that demonstrates *in vivo* tumor environment, where the liposomes have to translocate first across the endothelial barrier layer before reaching to the tumor target site. *In vitro* brain tumor model was treated for 24 h on day 21 and tumor cell viability was quantified on day 28. The percent tumor cell viability was observed to be decreased from 77.84 ± 1.57% for Dox-Erlo loaded plain liposomes to 47.85 ± 1.06% for DoxErlo loaded Tf-PFV liposomes for a 24 h treatment. Dox-Erlo encapsulated Tf-PFV liposomes decreased the percent tumor cell viability significantly ($p < 0.05$) as compared to single ligand or plain liposomes alone (Fig. 7A). Thus, the results showed an efficient co-delivery of Dox and Erlo from Tf-PFV liposomes across the endothelial barrier to the tumor cells in the scaffold. In addition, the fluorescence images of scaffold treated with Tf-PFV liposomes showed mostly dead tumor

cells in the scaffold section, which corroborates the excellent anti-tumor efficacy of dual functionalized liposomes over single or plain liposomes (Fig. 7B).

## 4. Conclusions

We have successfully designed and characterized Tf-PFV liposomes modified with Tf for receptor targeting and PFV to enhance cell penetration across the BBB. The dual functionalized liposomes showed significantly higher cellular uptake as well as increased transport of Dox and Erlo across co-culture barrier to glioblastoma tumor cells, resulting in enhanced tumor cell death inside scaffold and antitumor efficacy. The *in vitro* cell viability and hemolysis study demonstrates that Tf-PFV liposomes are suitable for *in vivo* administration. In addition, the dual functionalized liposomes exhibited clathrin-mediated cellular uptake as the major endocytosis pathway for their transport. Based on the promising results from *in vitro* studies, we anticipate that Tf-PFV liposomes will demonstrate to be an efficient delivery system in delivering anticancer chemotherapeutic agents across the BBB to the glioblastoma tumor specific site, *in vivo*.

## Supplementary Material

Refer to Web version on PubMed Central for supplementary material.

## Acknowledgements

This work was supported by National Institutes of Health (NIH) grant RO1 AG051574.

## Reference

[1]. Donahue MJ, Blakeley JO, Zhou J, Pomper MG, Laterra J, van Zijl PCM, Evaluation of human brain tumor heterogeneity using multiple T1-based MRI signal weighting approaches., Magn. Reson. Med 59 (2008) 336–344. [PubMed: 18183606]

[2]. Weil RJ, Palmieri DC, Bronder JL, Stark AM, Steeg PS, Breast Cancer Metastasis to the Central Nervous System, Am. J. Pathol 167 (2005) 913–920. [PubMed: 16192626]

[3]. Johnson DR, O'Neill BP, Glioblastoma survival in the United States before and during the temozolomide era., J. Neurooncol 107 (2012) 359–364. [PubMed: 22045118]

[4]. Lichter AS, Lawrence TS, Recent Advances in Radiation Oncology, N. Engl. J. Med 332 (1995) 371–379. [PubMed: 7824000]

[5]. Peer D, Karp JM, Hong S, Farokhzad OC, Margalit R, Langer R, Nanocarriers as an emerging platform for cancer therapy., Nat. Nanotechnol 2 (2007) 751–760. [PubMed: 18654426]

[6]. Prabhakar K, Afzal SM, Kumar PU, Rajanna A, Kishan V, Brain delivery of transferrin coupled indinavir submicron lipid emulsions-Pharmacokinetics and tissue distribution, Colloids Surfaces B Biointerfaces. 86 (2011) 305–313. [PubMed: 21565469]

[7]. Skarlatos S, Yoshikawa T, Pardridge WM, Transport of [125I]transferrin through the rat blood-brain barrier., Brain Res. 683 (1995) 164–171. [PubMed: 7552351]

[8]. Pardridge WM, Eisenberg J, Yang J, Human blood-brain barrier transferrin receptor, Metabolism. 36 (1987) 892–895. [PubMed: 3306281]

[9]. Cheng Y, Zak O, Aisen P, Harrison SC, Walz T, Structure of the Human Transferrin Receptor-Transferrin Complex, Cell. 116 (2004) 565–576. [PubMed: 14980223]

[10]. Qian ZM, Li H, Sun H, Ho K, Targeted drug delivery via the transferrin receptor-mediated endocytosis pathway., Pharmacol. Rev 54 (2002) 561–587. [PubMed: 12429868]

[11]. Sharma G, Lakkadwala S, Modgil A, Singh J, The Role of Cell-Penetrating Peptide and Transferrin on Enhanced Delivery of Drug to Brain, Int. J. Mol. Sci 17 (2016) 806.

[12]. Sharma G, Modgil A, Zhong T, Sun C, Singh J, Influence of short-chain cell-penetrating peptides on transport of doxorubicin encapsulating receptor-targeted liposomes across brain endothelial barrier, Pharm. Res 31 (2014) 1194–1209. [PubMed: 24242938]

[13]. Sharma G, Modgil A, Sun C, Singh J, Grafting of cell-penetrating peptide to receptor-targeted liposomes improves their transfection efficiency and transport across blood-brain barrier model, J. Pharm. Sci 101 (2012) 2468–2478. [PubMed: 22517732]

[14]. Kibria G, Hatakeyama H, Ohga N, Hida K, Harashima H, Dual-ligand modification of PEGylated liposomes shows better cell selectivity and efficient gene delivery, J. Control. Release 153 (2011) 141–148. [PubMed: 21447361]

[15]. Zong T, Mei L, Gao H, Cai W, Zhu P, Shi K, Chen J, Wang Y, Gao F, He Q, Synergistic dual-ligand doxorubicin liposomes improve targeting and therapeutic efficacy of brain glioma in animals, Mol. Pharm 11 (2014) 2346–2357. [PubMed: 24893333]

[16]. Bolhassani A, Potential efficacy of cell-penetrating peptides for nucleic acid and drug delivery in cancer, Biochim. Biophys. Acta - Rev. Cancer 1816 (2011) 232–246.

[17]. Rhee M, Davis P, Mechanism of uptake of C105Y, a novel cell-penetrating peptide., J. Biol. Chem 281 (2006) 1233–1240. [PubMed: 16272160]

[18]. Watkins CL, Brennan P, Fegan C, Takayama K, Nakase I, Futaki S, Jones AT, Cellular uptake, distribution and cytotoxicity of the hydrophobic cell penetrating peptide sequence PFVYLI linked to the proapoptotic domain peptide PAD., J. Control. Release 140 (2009) 237–244. [PubMed: 19409429]

[19]. Cai D, Gao W, He B, Dai W, Zhang H, Wang X, Wang J, Zhang X, Zhang Q, Hydrophobic penetrating peptide PFVYLI-modified stealth liposomes for doxorubicin delivery in breast cancer therapy., Biomaterials. 35 (2014) 2283–2294. [PubMed: 24360410]

[20]. Park JW, Bang E-K, Jeon EM, Kim BH, Complexation and conjugation approaches to evaluate siRNA delivery using cationic, hydrophobic and amphiphilic peptides, Org. Biomol. Chem 10 (2012) 96–102. [PubMed: 22045520]

[21]. Murray S, Rooprai H, Selway R, Pilkington G, A novel three-dimensional “all human” in vitro brain tumor invasion model, Neuro. Oncol 7 (2007) 307–308.

[22]. Meng W, Kallinteri P, a Walker D, Parker TL, Garnett MC, Evaluation of poly (glycerol-adipate) nanoparticle uptake in an in vitro 3-D brain tumor co-culture model., Exp. Biol. Med. (Maywood) 232 (2007) 1100–1108. [PubMed: 17720956]

[23]. Li X, Ding L, Xu Y, Wang Y, Ping Q, Targeted delivery of doxorubicin using stealth liposomes modified with transferrin, Int. J. Pharm 373 (2009) 116–123. [PubMed: 19429296]

[24]. Zhen Y, Thomas-Schoemann A, Sakji L, Boudou-Rouquette P, Dupin N, Mortier L, Vidal M, Goldwasser F, Blanchet B, An HPLC-UV method for the simultaneous quantification of vemurafenib and erlotinib in plasma from cancer patients., J. Chromatogr. B, Anal. Technol. Biomed. Life Sci 928 (2013) 93–97.

[25]. Rejman J, Bragonzi A, Conese M, Role of clathrin- and caveolae-mediated endocytosis in gene transfer mediated by lipo- and polyplexes., Mol. Ther 12 (2005) 468–474. [PubMed: 15963763]

[26]. Vercauteren D, Vandenbroucke RE, Jones AT, Rejman J, Demeester J, De Smedt SC, Sanders NN, Braeckmans K, The use of inhibitors to study endocytic pathways of gene carriers: optimization and pitfalls., Mol. Ther 18 (2010) 561–569. [PubMed: 20010917]

[27]. Nam HY, Kwon SM, Chung H, Lee S-Y, Kwon S-H, Jeon H, Kim Y, Park JH, Kim J, Her S, Oh Y-K, Kwon IC, Kim K, Jeong SY, Cellular uptake mechanism and intracellular fate of hydrophobically modified glycol chitosan nanoparticles., J. Control. Release 135 (2009) 259–267. [PubMed: 19331853]

[28]. Gaillard PJ, Voorwinden LH, Nielsen JL, Ivanov A, Atsumi R, Engman H, Ringbom C, de Boer AG, Breimer DD, Establishment and functional characterization of an in vitro model of the blood-brain barrier, comprising a co-culture of brain capillary endothelial cells and astrocytes., Eur. J. Pharm. Sci 12 (2001) 215–222. [PubMed: 11113640]

[29]. Lee D-W, Powers K, Baney R, Physicochemical properties and blood compatibility of acylated chitosan nanoparticles, Carbohydr. Polym 58 (2004) 371–377.

[30]. Fischer D, Li Y, Ahlemeyer B, Krieglstein J, Kissel T, In vitro cytotoxicity testing of polycations: Influence of polymer structure on cell viability and hemolysis, Biomaterials. 24 (2003) 1121–1131. [PubMed: 12527253]

[31]. Sharma G, Modgil A, Layek B, Arora K, Sun C, Law B, Singh J, Cell penetrating peptide tethered bi-ligand liposomes for delivery to brain in vivo: Biodistribution and transfection, J. Control. Release 167 (2013) 1–10. [PubMed: 23352910]

[32]. Ying X, Wen H, Lu W-L, Du J, Guo J, Tian W, Men Y, Zhang Y, Li R-J, Yang T-Y, Shang D-W, Lou J-N, Zhang L-R, Zhang Q, Dual-targeting daunorubicin liposomes improve the therapeutic efficacy of brain glioma in animals., J. Control. Release 141 (2010) 183–192. [PubMed: 19799948]

[33]. Lakkadwala S, Singh J, Dual Functionalized 5-Fluorouracil Liposomes as Highly Efficient Nanomedicine for Glioblastoma Treatment as Assessed in an In Vitro Brain Tumor Model., J. Pharm. Sci (2018). doi:10.1016/j.xphs.2018.07.020.

[34]. Xie Y, Ye L, Zhang X, Cui W, Lou J, Nagai T, Hou X, Transport of nerve growth factor encapsulated into liposomes across the blood-brain barrier: in vitro and in vivo studies., J. Control. Release 105 (2005) 106–119. [PubMed: 15893839]

[35]. Franke H, Galla H-J, Beuckmann CT, Primary cultures of brain microvessel endothelial cells: a valid and flexible model to study drug transport through the blood– brain barrier in vitro, Brain Res. Protoc 5 (2000) 248–256.

[36]. Rodal SK, Skretting G, Garred O, Vilhardt F, van Deurs B, Sandvig K, Extraction of cholesterol with methyl-beta-cyclodextrin perturbs formation of clathrin-coated endocytic vesicles., Mol. Biol. Cell 10 (1999) 961–974. [PubMed: 10198050]

[37]. Yao D, Ehrlich M, Henis YI, Leof EB, Transforming Growth Factor-β Receptors Interact with AP2 by Direct Binding to β2 Subunit, Mol. Biol. Cell 13 (2002) 4001–4012. [PubMed: 12429842]

[38]. Nakase I, Niwa M, Takeuchi T, Sonomura K, Kawabata N, Koike Y, Takehashi M, Tanaka S, Ueda K, Simpson JC, Jones AT, Sugiura Y, Futaki S, Cellular uptake of arginine-rich peptides: roles for macropinocytosis and actin rearrangement., Mol. Ther 10 (2004) 1011–1022. [PubMed: 15564133]

[39]. Antohi S, Brumfeld V, Polycation-cell surface interactions and plasma membrane compartments in mammals. Interference of oligocation with polycationic condensation., Zeitschrift Fur Naturforschung. Sect. C, Biosci 39 (1984) 767–775.

[40]. Zhu S, Qian F, Zhang Y, Tang C, Yin C, Synthesis and characterization of PEG modified N-trimethylaminoethylmethacrylate chitosan nanoparticles, Eur. Polym. J 43 (2007) 2244–2253.

[41]. Amin K, Dannenfelser R-M, In vitro hemolysis: Guidance for the pharmaceutical scientist, J. Pharm. Sci 95 (2006) 1173–1176. [PubMed: 16639718]

[42]. Janzer RC, Raff MC, Astrocytes induce blood–brain barrier properties in endothelial cells, Nature. 325 (1987) 253–257. [PubMed: 3543687]

[43]. Arthur FE, Shivers RR, Bowman PD, Astrocyte-mediated induction of tight junctions in brain capillary endothelium: an efficient in vitro model, Dev. Brain Res 36 (1987) 155–159.

[44]. Ishihara H, Kubota H, Lindberg RLP, Leppert D, Gloor SM, Errede M, Virgintino D, Fontana A, Yonekawa Y, Frei K, Endothelial cell barrier impairment induced by glioblastomas and transforming growth factor beta2 involves matrix metalloproteinases and tight junction proteins., J. Neuropathol. Exp. Neurol 67 (2008) 435–448. [PubMed: 18431253]

[45]. Bin Kim J, Three-dimensional tissue culture models in cancer biology, Semin. Cancer Biol 15 (2005) 365–377. [PubMed: 15975824]

**Highlights:**

- Transferrin-PFVYLI (Tf-PFV) liposomes were prepared by post-insertion method.
- Tf-PFV liposomes showed Tf receptor targeting and enhanced cell penetration.
- Cytotoxicity and hemolysis studies exhibited biocompatibility of the liposomes.
- Increased transport of Tf-PFV liposomes across the barrier into tumor-scaffold.
- Tf-PFV liposomes demonstrated excellent anti-tumor efficacy.

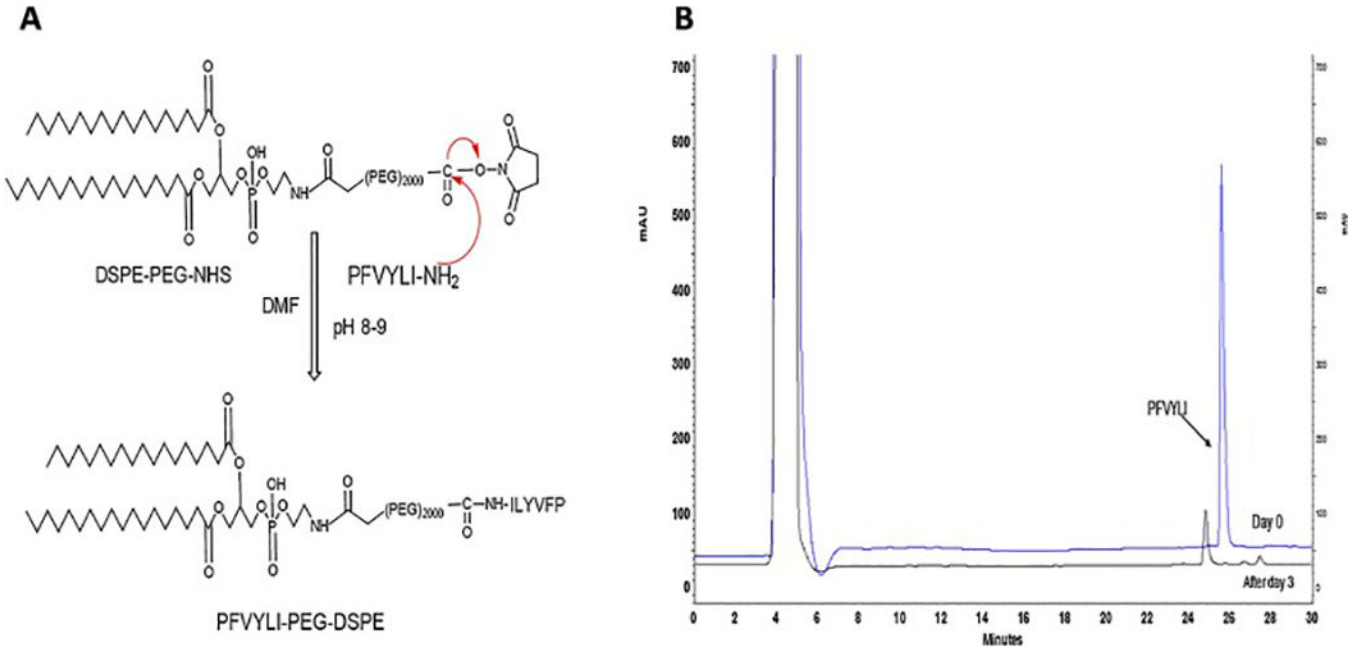


**Fig.1.**

(A) Schematic of the synthesis of PFV coupled to NHS-PEG$_{(2000)}$-DSPE. (B) HPLC spectra showing the rate of coupling of PFV to NHS-PEG$_{(2000)}$-DSPE.

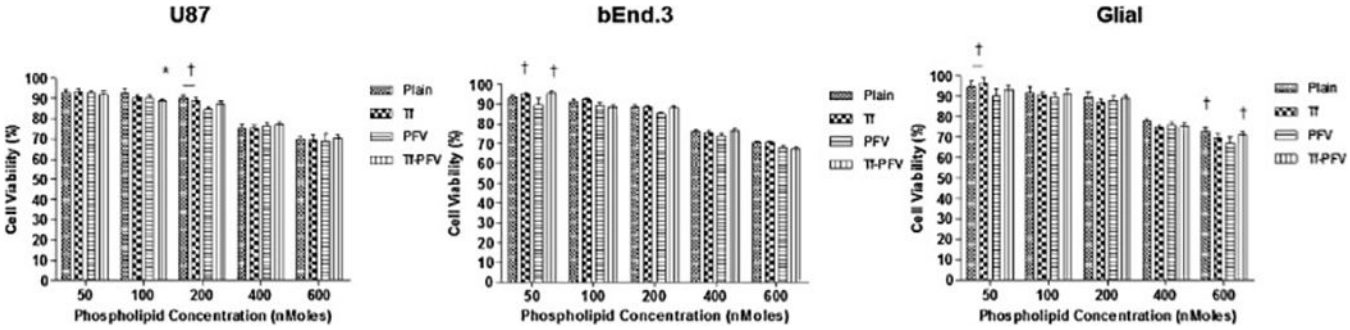


**Fig. 2.**

*In vitro* cell viabilities of U87, bEnd.3 and Glial cells after exposure to different phospholipid concentrations of plain, Tf, PFV, and Tf-PFV liposomes. Statistically significant ($p < 0.05$) differences is shown as (*) with plain liposomes and (†) with PFV-liposomes. Data represented as mean ± S.D., (n=4).

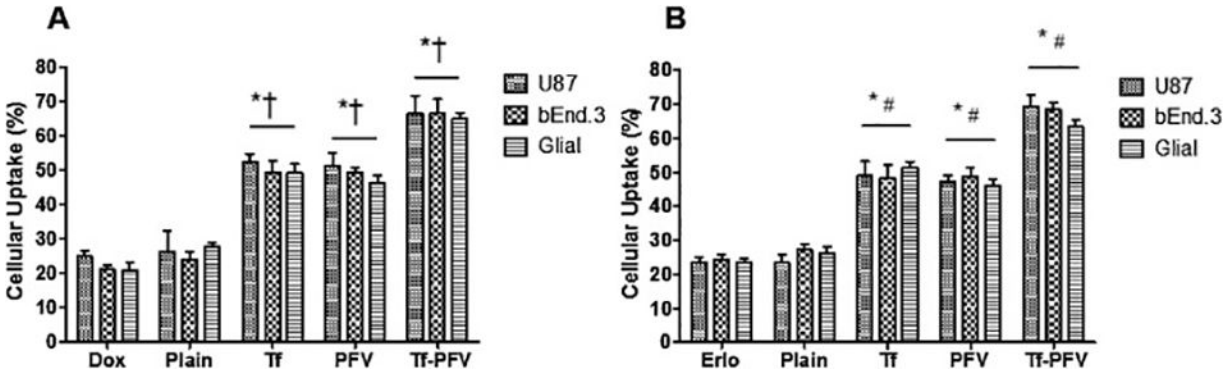


**Fig. 3.**

Graphs represent cellular uptake of A) Dox and B) Erlo encapsulated liposomes in U87, bEnd.3 and Glial cells after 2 h incubation. Data represented as mean ± SD, (n=4). Statistically significant ($p < 0.05$) differences is shown as (*) with plain liposomes, (#) with Erlo and (†) with Dox.

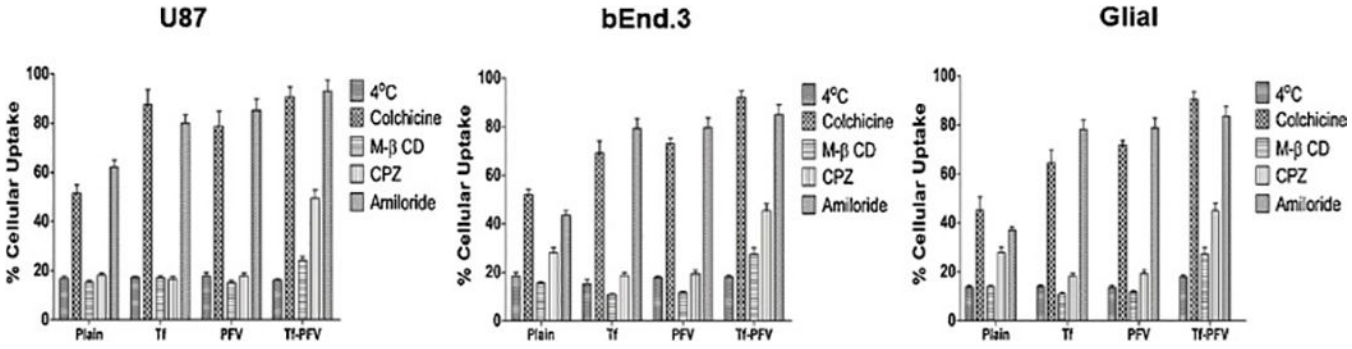


**Fig. 4.**

Graphs represent the effect of various inhibitors on the cellular uptake of coumarin-6 encapsulated liposomes in U87, bEnd.3 and Glial cells. The data are expressed as mean ± SD (n=4).

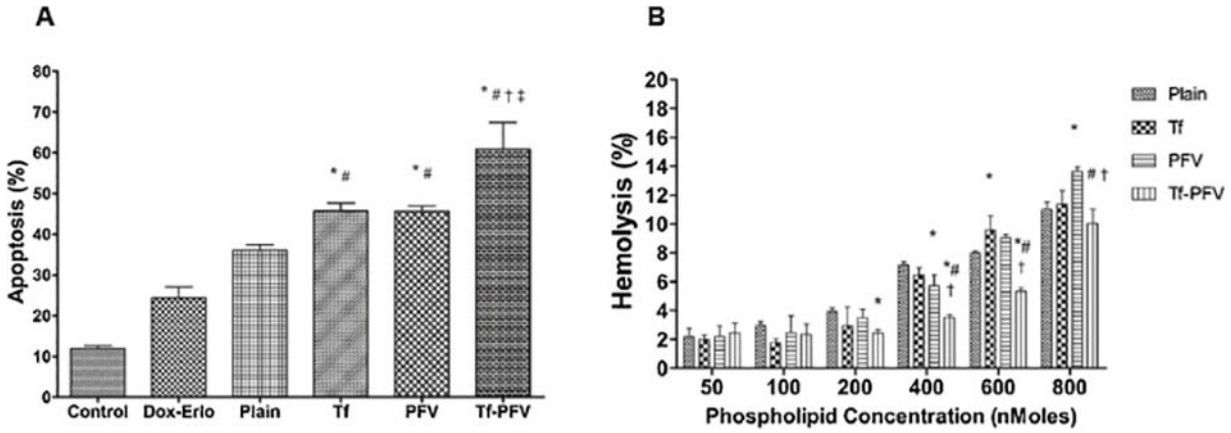


**Fig. 5.**

(A) Graph shows the proportion of apoptosis in U87 cells after treatment with Dox and Erlo encapsulated liposomes and free Dox -Erlo for 5 h. Statistically significant ($p < 0.05$) differences is shown as (*) with plain liposomes, (#) with free Dox-Erlo, (†) Tf-liposomes, and (‡) PFV-liposomes. (B) Percent hemolytic activity of various liposomes. Red blood cells were exposed to different liposomes at varying concentrations. Statistically significant ($p < 0.05$) differences is shown as (*) with plain liposomes, (#) with Tf-liposomes, and (‡) with PFV-liposomes. The data is represented as mean ± S.D. (n=4).

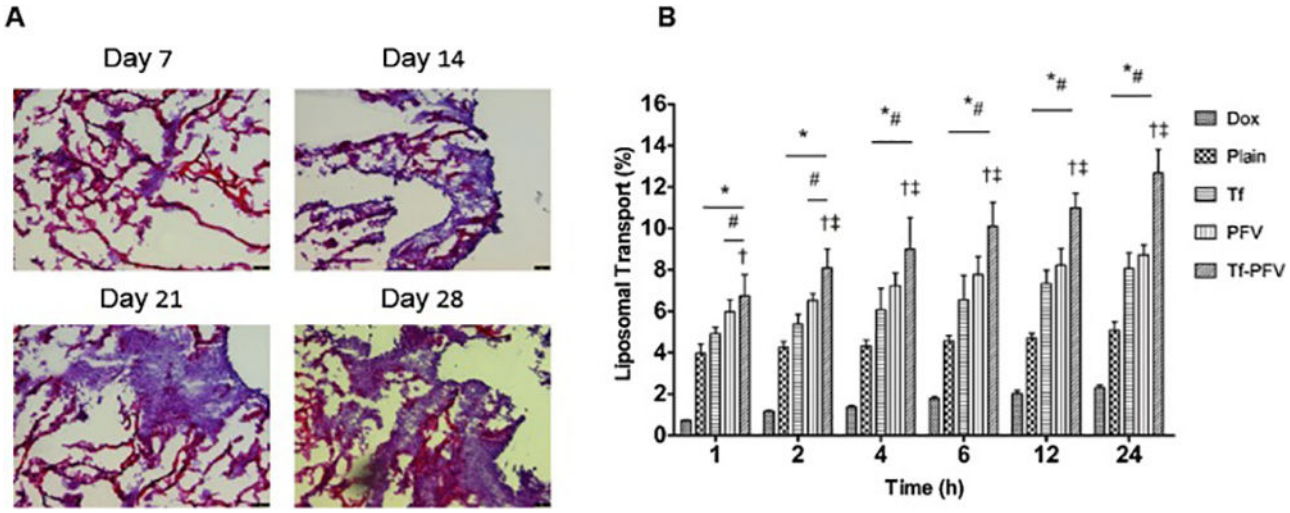


**Fig. 6.**

(A) At different time points, histological evaluation of tumor cell proliferation in PLGA-chitosan scaffold. The images show hematoxylin-eosin staining of scaffold sections with tumor cells growth (10x magnification). **(B)** Graph shows the percent transport of different liposomes encapsulated with doxorubicin, across *in vitro* brain tumor model. Significantly higher ($p < 0.05$) transport of Tf-PFV liposomes in comparison to plain liposomes was observed (*).Data represented as mean ± SD, (n=4).

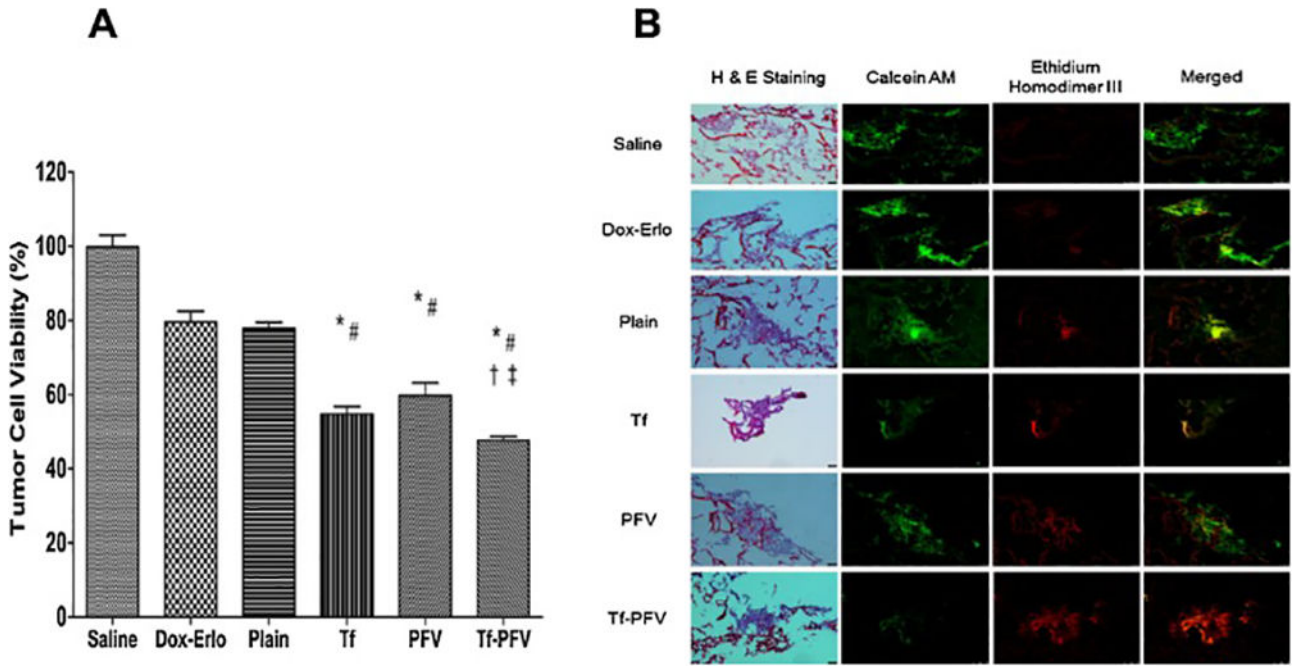


**Fig. 7.**

(A) Graph shows the percent tumor cell viability after 24 h treatment with different Dox and Erlo encapsulated liposomes after 24 h treatment using an *in vitro* brain tumor model. Statistically significant ($p < 0.05$) differences with (*) plain liposomes, (#) free Dox-Erlo, (‡) Tf-liposomes, and (†) PFV-liposomes was observed. Data represented as mean ± SD, (n=4). (B) The fluorescence images show tumor cell death in scaffold after treatment.

**Table 1.**

Particle size distribution, polydispersity index, zeta potential and entrapment efficiency of various liposomal formulations

| Liposomes | Particle size (nm) | PDI[a] | Zeta Potential (mV) | Dox EE[b] (%) | Erlo EE[b] (%) |
|---|---|---|---|---|---|
| Plain | 165.05 ± 3.75 | 0.182 ± 0.040 | 5.33 ± 0.66 | 63.47 ± 3.02 | 54.06 ± 1.34 |
| Tf | 163.40 ± 6.07 | 0.221 ± 0.033 | −5.26 ± 1.20 | 65.55 ± 3.05 | 54.03 ± 2.66 |
| PFV | 158.70 ± 1.45 | 0.210 ± 0.021 | 14.16 ± 1.48 | 65.08 ± 1.10 | 53.92 ± 1.97 |
| Tf-PFV | 161.90 ± 4.60 | 0.232 ± 0.011 | 7.66 ± 0.87 | 65.26 ± 1.89 | 53.99 ± 1.63 |

[a]Polydispersity index (PDI).

[b]Entrapment efficiency (EE). The data represented as mean ± SD, (n=4).